DOI 10.1007/s11029-017-9637-0
Mechanics of Composite Materials, Vol. 53, No. 1, March, 2017 (Russian Original Vol. 53, No. 1, January-February, 2017)

DYNAMIC CHARACTERIZATION OF AN ALL-FRP BRIDGE

C. Casalegno* **and S. Russo**

Keywords: *pultruded FRP bridge, dynamic testing, experimental modal analysis, vibration serviceability, resonance*

The light weight and high deformability of bridges made with pultruded FRP (fiber-reinforced polymer) materials make them very promising, but, at the same time, vulnerable to dynamic loadings. As a consequence, the vibration serviceability limit state can govern their design. There is currently a lack of data about the dynamic characteristics of FRP bridges and of design guidelines for securing their vibration serviceability. The paper presents the results of dynamic testing and characterization of an all-FRP spatial footbridge. The main modal parameters of the bridge are evaluated by an experimental modal analysis and by comparison of experimental data with FE analysis results. The identified flexural and torsional modes of the bridge are characterized by relatively high values of frequencies and damping. Results of the dynamic characterization give useful information about the dynamic characteristics of this kind of structures and can contribute to the elaboration of future guidelines for providing them with the vibration serviceability.

1. Introduction

The use of pultruded FRP (fiber-reinforced polymer) materials in structural engineering has rapidly increased in the last few decades. A field in which this material founds several applications is the building of bridges, footbridges is particular. For designers and bridge owners, pultruded FRP materials offer distinct advantages over other materials that can provide dynamic solutions and such long-term benefits as a reduced mass, leading to easier, faster and more economic installations, the reduction of seismic actions, and a superior durability, in particular, to the atmospheric degradation, to the action of deicing salts, etc. [1].

All-FRP bridge structures are usually realized with superstructures constructed exclusively fromof FRP profiles, while the substructure elements (abutments and piers) usually consist of traditional materials. FRP structural profiles are commonly pultruded, even if other kind of processes, such as filament winding and bag molding, could be employed. The standard profiles,

IUAV University of Venice, Department of Design in Complex Environment, Dorsoduro 2206, 30123 Venice, Italy
*Corresponding author; e-mail: casalegno.c@gmail.com

Russian translation published in Mekhanika Kompozitnykh Materialov, Vol. 53, No. 1, pp. 27-46, January-February, 2017. Original article submitted March 11, 2016.

with shapes similar to those used in structural steelworks, have continuous fibers running only in the longitudinal direction and dispersed between layers of mats of fibers [2]. The material is characterized by very high values of strength in the pultrusion direction, which is the longitudinal one, with a tensile strength higher than 200 MPa, accompanied by relatively low values of the elastic modulus, which are in the range of 20-30 MPa. Due to the longitudinal fiber orientation, both the strength and the elastic moduli are significantly lower in the transverse direction.

The light weight, high deformability, and low damping of FRP structures make them vulnerable to such dynamic loadings as wind excitation and, especially, human-induced vibrations. As a consequence, the vibration serviceability can govern their design. The problem gets particularly topical in the case of FRP footbridges, for which human-induced dynamic loadings are becoming increasingly important in the cases of their long spans and high slendernesses. The problem of excessive human-induced vibrations of footbridges has been raised in many cases in the past [3], and it attracted a great public and professional attention after the Millennium Bridge in London had to be closed in the June of 2000, just two days after its opening, due to the unexpected lateral vibration caused by the resonance of natural frequencies of the structure with the dominant frequencies of the human-induced load. Excessive vibrations may arise in footbridges if at least one of their natural frequencies coincides with the first or second harmonic of human activity. Among all activities, walking is the most frequent type of actions on footbridges. The pacing rate of humans typically ranges from 1.4 to 2.5 Hz, resulting in a second harmonic of the force having frequencies up to 5 Hz [3]. As a consequence, most of the design codes and guidelines for footbridges prescribe minimum values of the natural frequencies of the structures of about 3 to 5 Hz [4], which may not be achieved for lightweight FRP bridges.

Although the static behavior of pultruded FRP elements and structures is nowadays studied thoroughly (see [5-9] among others), their dynamic behavior is considered only in a few studies [10-15], and only a few studies concern the dynamic performance of FRP bridges [16-19] (in [16-17], in particular, FRP footbridges, are analyzed). Due to the shortage of data on the vibration performance of FRP structures and the lack of guidelines for securing their vibration serviceability, a conservative approach, without any reference code, has to be adopted in the design of FRP footbridges, which does not allow the full exploitation of the advantages related to the use of this new material.

This paper presents the results of dynamic tests carried out on a truss-type bolted pultruded FRP footbridge. A dynamic identification of the structure is carried out using an experimental modal analysis and comparing the data obtained with FE analysis results in order to determine the main natural frequencies, damping ratios, and modal shapes of the bridge. The results of the dynamic characterization give useful information about the dynamic characteristics of this kind of structures and can contribute to the elaboration of future guidelines for providing them with the vibration serviceability.

2. Description of the Structure

The pultruded FRP footbridge considered in the present study (Fig. 1) was built in 2011 in Prato (Italy) as a bicycle and pedestrian crossing of the main street connecting the north and south parts of the city. The bridge is realized through a spatial truss structure made from two pultruded FRP truss beams of span 25 m mutually connected by bottom and chords and supported by reinforced concrete walls about 5.5 m high.

The bottom and top chords are curved both in the vertical and horizontal planes. In particular, the bottom and top chord has a maximum uplift at the midspan of about 35 cm, while the bridge width varies from 2.5 m at the midspan to about 3.6 m at its supports (see Fig. 1). The curvature of the chords was used to increase the global stability of the structure, and, in particular, its torsional performance. The bridge deck is made from ribbed FRP panels (h = 4 cm, m = 17 kg/m^2, and E = 23,000 MPa) treated superficially in order to achieve the necessary roughness imposed by safety requirements. Two fixed supports are at one end of the bridge and two unidirectional sliding ones at the other end, realized with Teflon sheets. Two truss structures, made from pultruded FRP shapes, are placed side by side to the RC walls to accommodate elevators and to support cantilevered stairs. The webs of the trusses are all realized by coupling pultruded FRP channel (C) profiles connected by steel plates and steel bolts (Fig. 1). In particular, the bottom and top chords are made from two C-profiles 300 mm high. The vertical struts and the tensed diagonals are made from two Cs of height 120 mm. The compressed diagonals at the midspan are made from two Cs

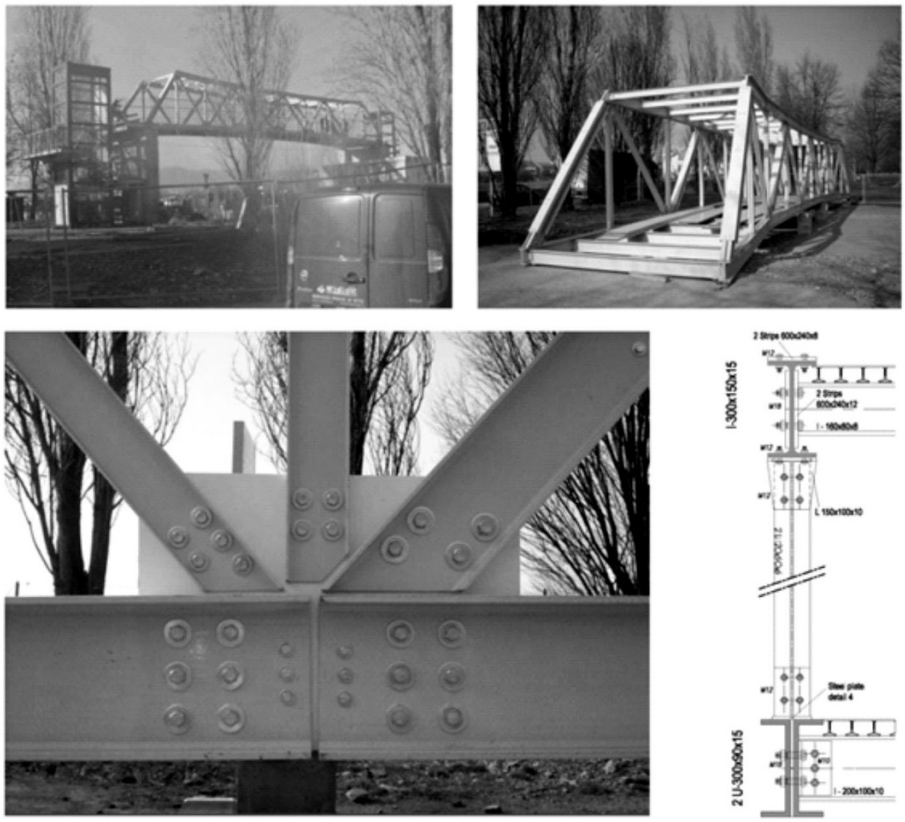

Fig. 1. A GFRP footbridge.

200 mm high, the intermediate compressed diagonals — from four Cs 200 mm high, and those at the ends — from four Cs of height 240 mm. The transverse beams connecting the bottom longitudinal chords are made from I-profiles of height 200 mm, while I-profiles 160 mm high are used to connect the upper chords. The horizontal bracings are made from flat sheets120 mm wide and 10 mm thick. The mean mechanical characteristics of the FRP profiles employed, as declared by the manufacturer, were as follows: density 1700 g/m^3, longitudinal tensile strength 300 MPa, longitudinal elastic modulus 25,000 MPa, transverse elastic modulus, 8500 MPa, shear modulus 3000 MPa, longitudinal Poisson ratio 0.23, and transverse Poisson ratio 0.09.

3. Test Setup

Experimental tests under ambient and forced excitations were carried out. The dynamic testing was conducted using nine piezoelectric accelerometers PCB M19A (sensitivity 1 V/g, range ± 5 g, resolution $1 \cdot 10^{-5}$ g, and frequency range 0.025-800 Hz).

The design of test configuration envisaged five accelerometers in the vertical, three in the transverse, and one in the longitudinal direction, arranged in one accelerometer tern, two accelerometer couples, and two single sensors (see Fig. 2). The accelerometer tern included one accelerometer placed in the vertical direction, one in the transverse direction, and one in the longitudinal direction. The accelerometer couple included one accelerometer placed in the transverse direction and one in the vertical direction. The two single accelerometers were placed in the vertical direction. Three different acquisition setups were used, as illustrated in Fig. 2 and described in Table 1 with details of the type of excitation. A prior acquisition of data at ambient vibrations was first carried out, and then the structure was subjected to forced excitations induced by movements of a person. The signal was acquired without preprocessing, with a sampling rate of 256 Hz.

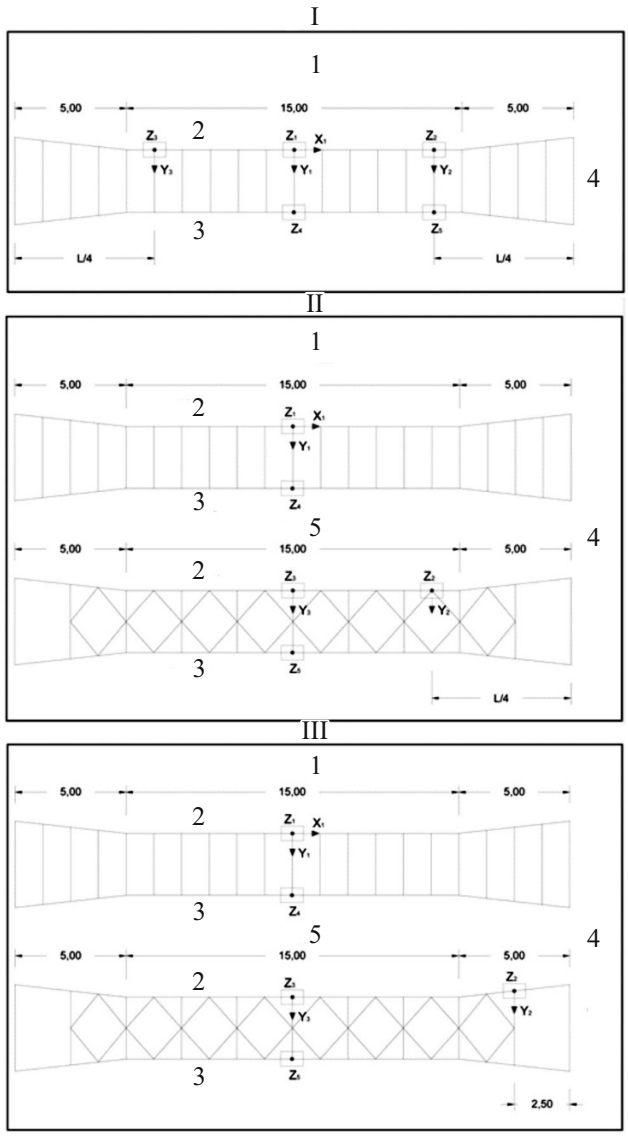

Fig. 2. Acquisition setups.

4. Dynamic Identification

A dynamic identification of the structure was carried out through an experimental modal analysis of free-decay signals relative to forced excitations. The well-known Eigensystem Realization Algorithm (ERA) method [20] was adopted. The algorithm was implemented in the Matlab®.

In particular, the free-decay signals from setup acquisitions 2, 3, 4, and 8 were used in the identification procedure.

The mean and trend were removed from the signals, and they were filtered with a band-pass filter between 1 and 30 Hz.

The identification was carried out varying the model order from $m = 6$ to 100. In order to distinguish between the real and numerical modes, results of the identification procedure were plotted as frequency vs. model order (see Fig. 3) and frequency vs. damping diagrams (see Fig. 4). In fact, the real modes of the structure were characterized by a low variability of the modal parameters (e.g., the frequency and, to a lesser extent, damping) at increasing values of model order. In Fig. 3, the presence of a real mode is demonstrated by the stability of frequency with increasing model order. In Fig. 4, the natural frequencies

TABLE 1. Type of Excitations Used in Different Acquisition Setups

Acquisition	Excitation	Setup
1	Ambient vibrations	1
2	Jump of a person at the midspan, at the center of deck	
3	Swaying at the midspan, at the center of deck	
4	Swaying at the midspan, at the right side of deck	
5		
6	Swaying at $L/4$, at the center of deck	
7	Horizontal push on a vertical strut, at the midspan, at the right side	
8	Horizontal push on a vertical strut, at the midspan, at the right side	2
9		
10	Push on the second diagonal from the acquisition station side	
11	Push on the first diagonal from the acquisition station side	3
12		
13		

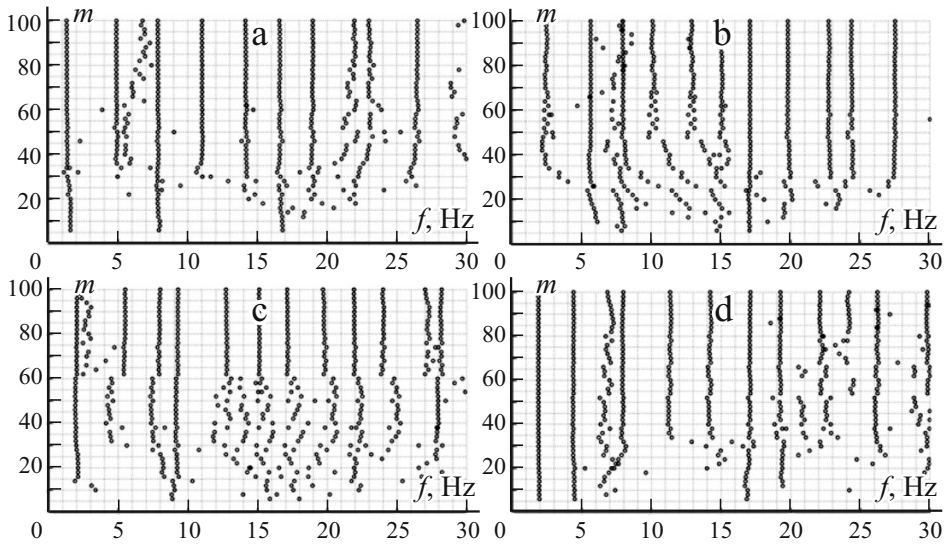

Fig. 3. Model order vs. frequency, acquisitions 2 (a), 3 (b), 4 (c), and 8 (d).

form clusters of points within a small range of frequencies and damping values due to the low variability of these parameters. Clusters in a realistic frequency range (usually 0-5%) are considered as indicative of the presence of a mode of the structure.

In Figs. 5-8, the power spectral density (PSD) of signals in relation to the four acquisitions considered are presented, while in Fig. 3 and 4, the scatter plots of frequencies vs. model order and damping, respectively, are shown. The signal in the longitudinal direction of the bridge (X1 in Figs. 2) was not considered in the analysis, because its contribution was not expected to be very significant for the dynamic identification procedure.

A FE model of the structure was also realized using the Oasys GSA® software (Fig. 9). The model was meshed with beam elements with account of the shear deformability. The internal restraints were modeled as fully fixed, considering the configuration of the joints (Fig. 1). A modal analysis was also carried out. The masses considered were those of the FRP profiles and the FRP panels forming the deck. Different options were tried for the restraints at the unidirectional sliding supports, owing to doubts about the actual behavior of the supports and to the difficulties encountered in matching the experimental

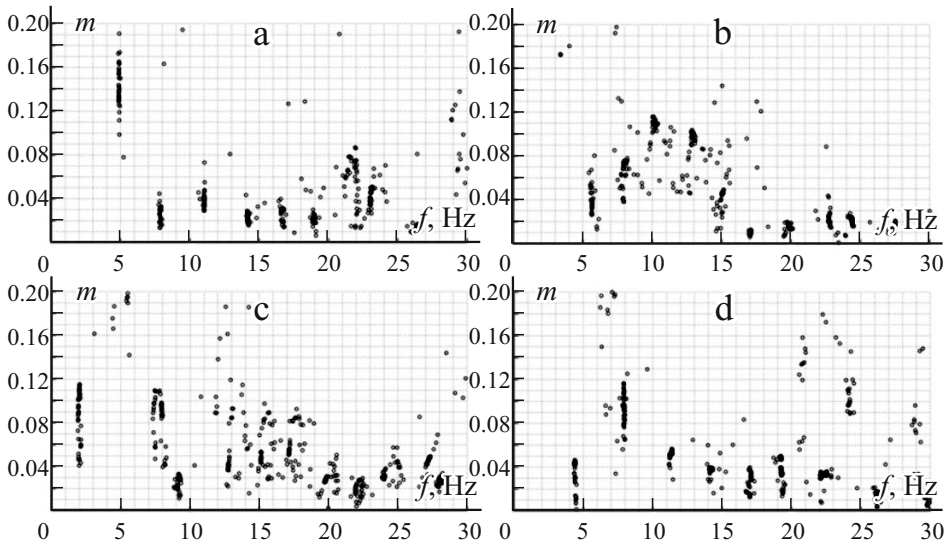

Fig. 4. Damping vs. frequency, acquisitions 2 (a), 3 (b), 4 (c), and 8 (d).

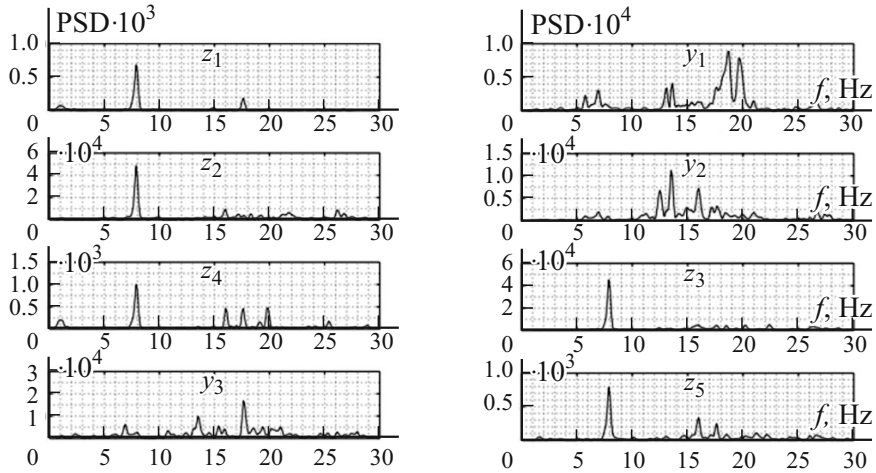

Fig. 5. PSD of acquisition 2.

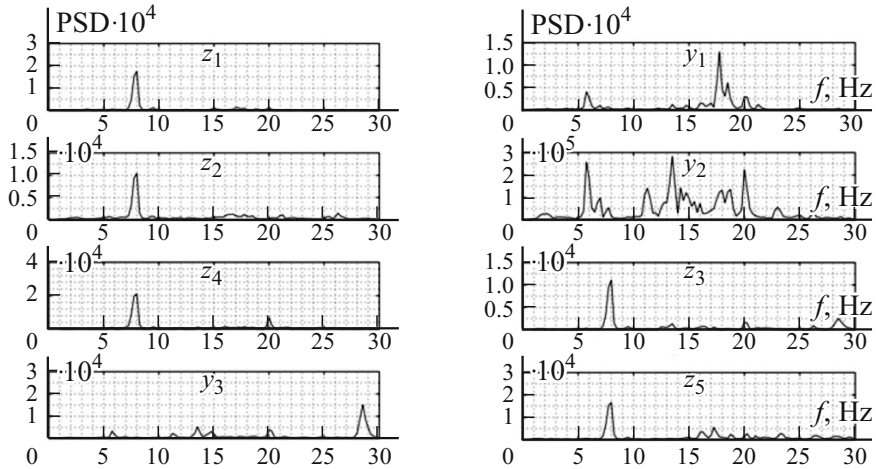

Fig. 6. PSD of acquisition 3.

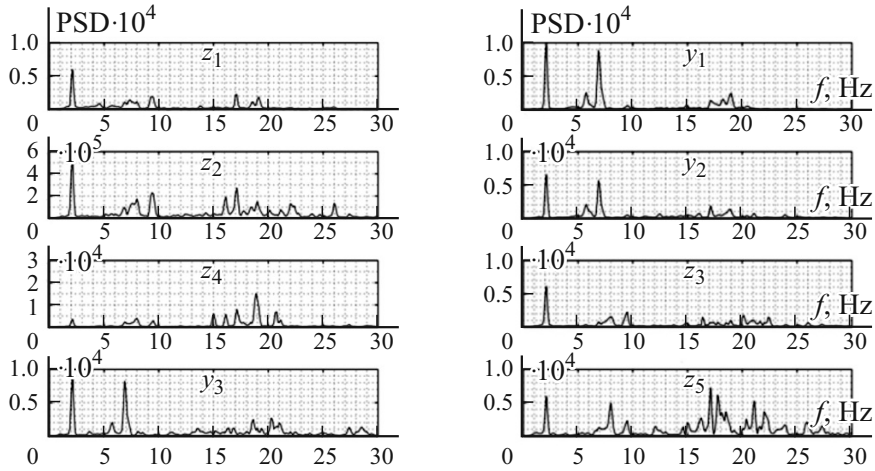

Fig. 7. PSD of acquisition 4.

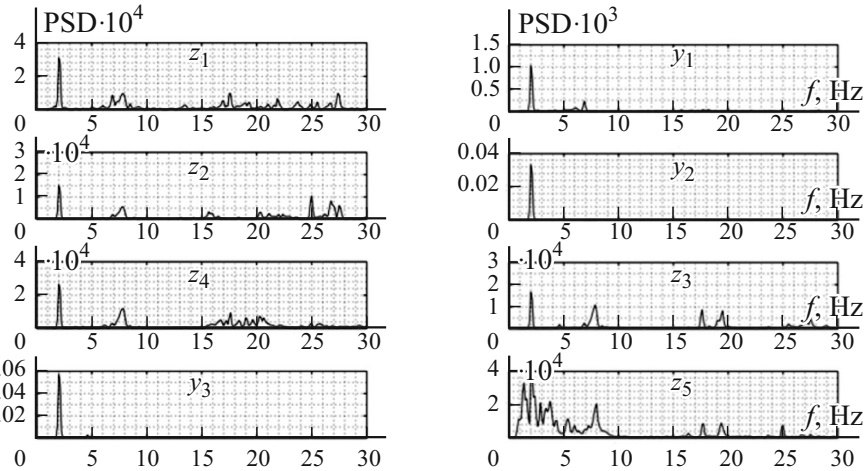

Fig. 8. PSD of acquisition 8.

modal parameters with those of the FE model. In particular, three different conditions were considered: with restricted i) vertical and transverse displacements, ii) all displacements, and iii) only vertical displacements. From a first comparison between experimental and numerical results, a better agreement was obtained for condition iii), which was finally adopted in the model. The characteristics of the first 11 vibration modes of the FE model are summarized in Table 2, but in Figs. 10-11, mode shapes are represented.

The comparison of experimental and numerical results made it possible to identify the main modal parameters of the bridge. In particular, modes 1, 2, 3, 5, 6, 8, and 10 of Table 2 were identified, although doubts about some of the results still remained, as described in what follows.

Mode 1 was a lateral vibration mode related to the lateral sliding of supports (Fig. 10). It is visible both in the peaks at about 2.0 Hz of the PSD of the signals of acquisition 4 (Fig. 7) and in the stable experimental frequency f_{exp} in the model order vs. frequency diagram of the same acquisition (Figs. 3c). In the damping vs. frequency diagram (Fig. 4c), the mode presents values of damping ξ of about 10-11%. These values are very high and are probably related to the damping associated with sliding on the Teflon support. The experimental mode shape is represented in Fig. 12, where it is viewed from the top. The instrumented nodes, that is, those for which the modal displacements were computed, are seen. This mode shape was extracted from acquisition 4, with setup 1 (Fig. 2), so only modal displacements of some nodes of the deck are available.

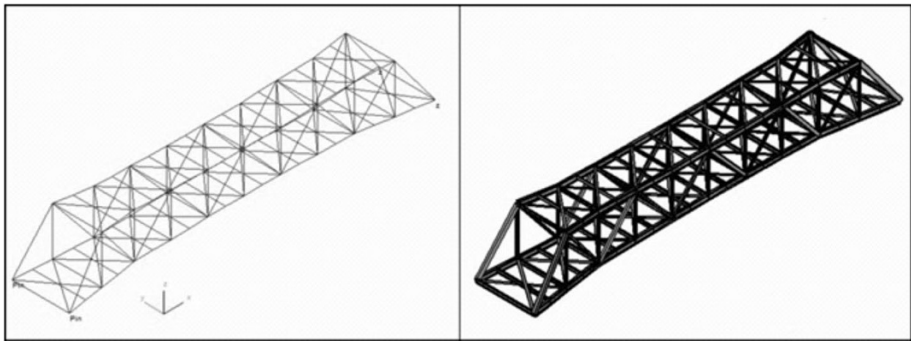

Fig. 9. FE model of the bridge.

TABLE 2. Results of the FE Modal Analysis

Mode	Frequency, Hz	Description
1	2.0	Lateral movement
2	4.2	1st distorsional mode
3	6.8	1st flexural mode
4	7.2	2nd distorsional mode
5	9.0	1st torsional mode
6	11.9	1st mode of lateral deflection
7	17.7	2nd torsional mode
8	17.8	2nd flexural mode
9	20.1	Spurious mode
10	21.8	2nd mode of lateral deflection
11	22.0	3rd flexural mode

In the representation of experimental mode shapes, the transverse displacement (in the *Y*-direction) at both sides of the deck were assumed the same, because accelerations in this direction where registered only at one side. Some doubts exist about this experimental mode. In fact, the FE mode shape presents horizontal displacements increasing from the fixed extremity of the bridge to the extremity with sliding supports, but it is not the same for the experimental mode shape (Fig. 10). Moreover, quiet significant displacements in the vertical direction were also obtained for the experimental mode shape. In general, a larger number of acquisition points would have allowed a better representation and evaluation of the experimental mode shapes.

Mode 2 was distorsional in which the upper part of the bridge moved laterally with respect to the deck (Fig. 10). In the results of identification, the mode was evidenced by a stable frequency of about 4.4 Hz in the model order vs. frequency diagram of acquisition 8 (Fig. 3d) and by a cluster of points around this frequency value in the damping vs. frequency diagram (Fig. 4d). From the latter diagram, it is seen that the damping relative to this mode was about 4.5%. The experimental mode shape extracted from acquisition 8 with setup 2 (Fig. 2) is represented in Fig. 12 and shows the lateral deflection of the upper part of the bridge, which is in good agreement with that extracted from the FE model (Fig. 10).

Mode 3 was the firstt flexural mode of the bridge (Fig. 10). The mode was clearly evident at a frequency of about 7.8 Hz in the PSD and in the model order vs. frequency and damping vs. frequency diagrams relative to acquisition 2 (Figs. 5, 3a and 4a, respectively). The damping was about 3%. The experimental mode shape is presented in Fig. 12. Besides the flexural deformation of the deck, some displacements in the transversal direction arouse, and the deck inclined in the transversal direction, but these displacements were relatively small compared with the downward deflection of the deck. In judging the mode shape, it must be considered that the node opposite to that with sensors Y3 and Z3 was not instrumented in the acquisition setup (setup 1, Fig. 2), so the node did not show a downward movement, as it could be expected.

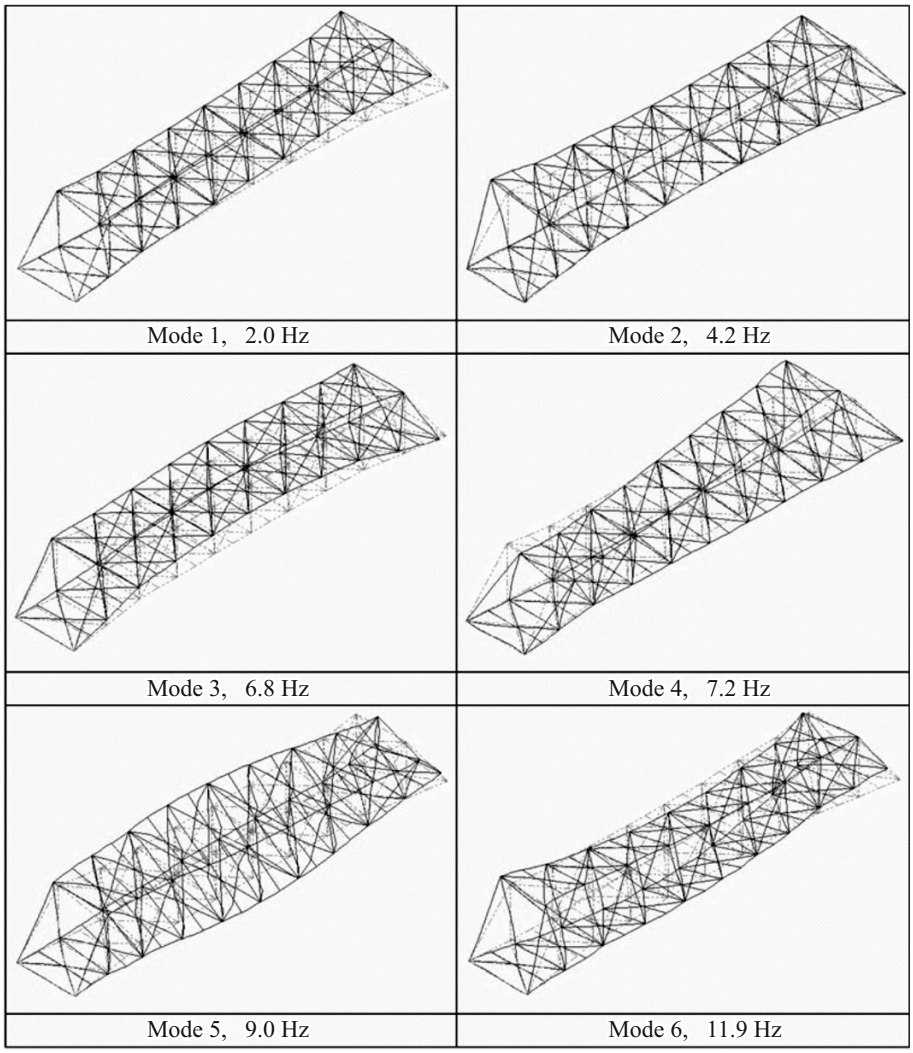

Fig. 10. Modes 1-6 extracted from the FE model.

Mode 5 was the first torsional mode of the structure (Fig. 10). It was visible in the diagrams relative to acquisition 4 (Figs. 7, 3c and 4c) at a frequency of about 9.3 Hz. The damping was about 3%. The experimental mode shape is presented in Fig. 12. A good agreement was obtained between the experimental mode shape and that extracted from the FE model (Fig. 10), taking into account that, in this case too, the node opposite to that with sensors Y3 and Z3 did not show any vertical movement, because it was not instrumented in the acquisition setup.

Mode 6 was the first mode of lateral deflection of the bridge (Fig. 10). The mode is visible in the model order vs. frequency diagram and in the damping vs. frequency diagram relative to acquisition 2 (Figs. 3a and 4a) at a frequency of 11 Hz. The damping was about 4%. The experimental mode shape is presented in Fig. 12.

Mode 8 was the second flexural model of the bridge (Fig. 11). The mode was visible in diagrams of different acquisitions and is particularly evidenced by the cluster of points at a frequency of about 17.1 Hz in the damping vs. frequency diagram of acquisition 3 (Fig. 4b). A relatively low damping ratio, equal to about 1%, was found for this mode. The experimental mode shape is presented in Fig. 12. As usually, the absence of displacements for the nodes not instrumented have to be taken into account in judging of the mode shape and in comparison with those extracted from the FE model.

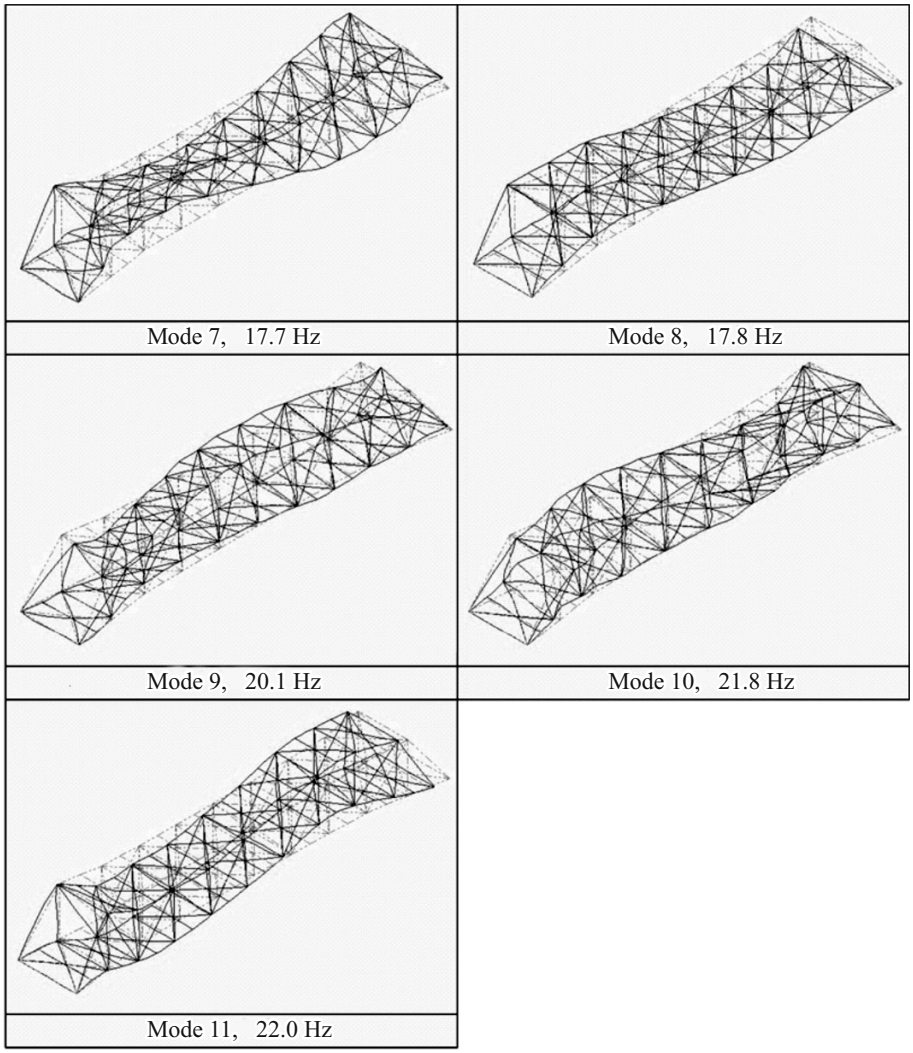

Fig. 11. Modes 7-11 extracted from the FE model.

TABLE 3. Results of Identification and Comparison with FEA Results

Mode	Frequency, Hz		Damping, %	Description
	FEM	Experimental	Experimental	
1	2.0	2.0	10-11	Lateral movement
2	4.2	4.4	4.5	1st distorsional mode
3	6.8	7.8	3	1st flexural mode
5	9.0	9.3	3	1st torsional mode
6	11.9	11.0	4	1st mode of lateral deflection
8	17.8	17.1	1	2nd flexural mode
10	21.8	21.9	2	2nd mode of lateral deflection

Finally, mode 10 was the second mode of lateral deflection of the bridge (Fig. 11). The mode was visible in the model order vs. frequency diagram and in the damping vs. frequency diagram of acquisition 4 (Figs. 3c and 4c). The damping was about 2%. The experimental mode shape is represented in Fig. 12.

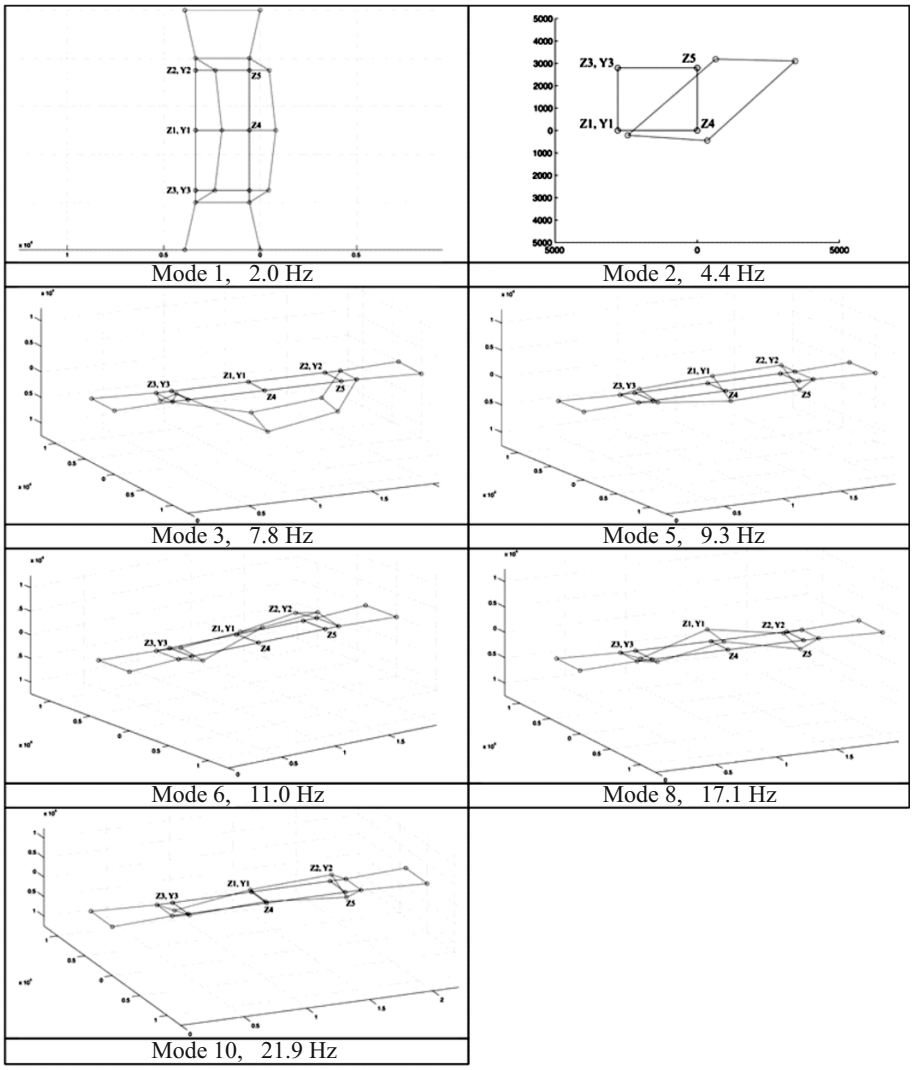

Fig. 12. Experimental mode shapes.

In Table 3, the identified modal parameters are summarized, and the natural frequencies are compared with those obtained from the FE analysis. A reasonable agreement is seen between the identified experimental natural frequencies and those of the FE model. This fact supports the validity of the results of the experimental modal analysis.

5. Discussion of Results and a Comparison with the Dynamic Behavior of Other Footbridges

A comparison between the experimentally identified natural frequencies and the prescriptions given by Eurocode 0 [4] can be carried out. For footbridges, the standard specifies a minimum frequency of 5 Hz for vertical vibrations and a minimum frequency of 2.5 Hz for lateral and torsional ones. For higher values of natural frequencies, a verification of the comfort criteria (the maximum acceptable acceleration) is not required. For the FRP bridge analyzed, the frequencies of the first flexural, torsional, and lateral modes were 7.8, 9.3, and 11 Hz, respectively. Thus, the standard requirements were largely satisfied. The frequencies of the first torsional and lateral modes were significantly higher than the prescribed minimum. In spite of the high deformability of the FRP material, the natural frequencies were high, probably due to the spatial truss type of the bridge, which was rather rigid with respect to bending and torsional deformations.

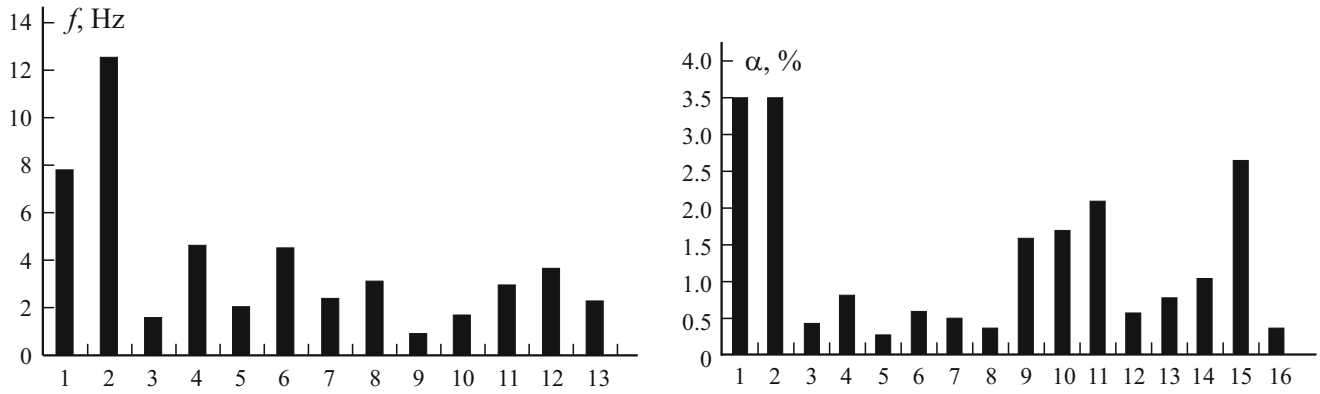

Fig. 13. Comparison of natural frequency f and damping α of some footbridges.

TABLE 4. Comparison of Modal Properties of Different Footbridges

Bridge	Main span, m	Structural system	f, Hz	Damping, %
Present bridge	25	Space truss, all-FRP	7.8 (1st vertical) 9.3 (1st torsional) 11.0 (1st lateral)	3-4
Pontresina bridge	12.5	Truss girder	4.18 (1st lateral) 12.54 (1st vertical)	3-4
Aberfeldy bridge	63	Cable-stayed, all-FRP	1.52 (1st vertical)	0.42
EMPA bridge	15.6	Cable-stayed FRP laboratory bridge	4.62 (1st vertical)	0.80
Podgorica bridge	78	Cable-stayed, steel box girder	2.04 (1st vertical)	0.26
Sheffield bridge	10.8	Pre-stressed simple beam, reinforced concrete	4.50 (1st vertical)	0.60
Warwick bridge	16.2	Steel-concrete composite laboratory structure	2.40 (1st vertical)	0.50
Burlington bridge	54.7	Cable-stayed, steel	3.10 (1st vertical) 4.62 (1st torsional)	0.22-0.53
Dolerw bridge	50	Suspended, steel	0.89 (1st vertical) 2.22 (1st lateral) 3.24 (1st torsional)	0.50-2.68
Singapore bridge	35	Suspended, steel	1.7 (1st vertical)	1.0-2.4
Reutigen bridge	54	Space truss, wood	1.66 (1st lateral) 2.94 (1st vertical) 3.98 (1st torsional)	1.3-2.9
[11]	19.9	Precambered steel-concrete composite beam	3.67 (1st vertical)	0.40-0.73
Bridge in UK	34	Prestressed concrete ribbon	2.3 (1st vertical)	0.53-1.02
Millennium bridge	144	Suspended, steel	-	0.76-1.30
[14]	30	Stressed ribbon, concrete	-	1.7-3.6
Hungerford Millennium Bridge	53	Multicable-stayed, reinforced concrete	-	0.21-0.51

In Table 4, the main identified modal parameters are compared with those of other footbridges made from traditional structural materials or from FRP, and in Fig. 13, the natural frequencies f of the first vertical mode and the mean damping values a of the first vertical, torsional, and lateral modes, where available, are compared. The modal parameters of the bridges were taken from [3, 16, 17] and the references reported in [3]. From the table and histograms, it can be observed that the natural frequencies of the bridge analyzed were significantly higher, more than two times in most cases, than those of the other bridges.

The frequencies of the first torsional, and especially of the first lateral mode, were particularly high. The estimated damping values of about 3-4% of the first vertical, torsional, and lateral modes were also rather high compared with those reported in the literature, which are in the range of about 0.2-4%. Anyway, it should be considered that some of the compared bridges are quite different from that analyzed here, being realized with different materials and with a different structural types. The damping values obtained for the present bridge are in good agreement with those of the Pontresina FRP bridge, which is a GFRP bridge very similar to that analyzed here. This fact supports the validity of present results.

In general, it can be concluded from the analysis results that the bridge performs well from the dynamical point of view. However, it would be good to evaluate the vibration response of the bridge in terms of maximum values of acceleration under service conditions in order to check the fulfillment of the comfort criteria defined in international standards. In fact, the reduced mass of the FRP structure could result in high values of the maximum accelerations, as also reported in [16].

Finally, it should be noted that a larger number of sensors would have been necessary in order to conduct a more complete and reliable dynamic identification. In fact, doubts still remain about some of the mode shapes identified, as already mentioned previously. Also, in the various diagrams presented in the paper, the presence of some other possible experimental modes is evidenced by stable frequencies with realistic values of damping. For these modes, the experimental mode shape was not clear, and a correspondence with FE analysis results was not found. Anyway, the principal natural modes, that is, those of most interest from the engineering point of view (the first vertical, torsional, and lateral modes), have been identified quiet clearly.

6. Conclusions

Due to their low mass, high slenderness, and high deformability, FRP footbridges are usually sensitive to dynamic excitations. The design of such structures may probably be governed by the vibration serviceability, but there is currently a lack of data on the dynamic properties of FRP pedestrian bridges, as well as in guidance documents on vibration serviceability of designs. The paper presented results of the dynamic characterization of a FRP footbridge, contributing to the deepening of the knowledge of the dynamic characteristics of this kind of structures and to the definition of possible guidelines for securing the vibration serviceability.

In particular, the parameters relative to six modes of the bridge have been identified by an experimental modal analysis and a comparison with results of a FE analysis.

From results of the analysis performed, the following conclusions can be drawn.

- The natural frequencies of the bridge relative to the principal modes (the first vertical, torsional, and lateral modes) were rather high, — significantly higher than the minimum required by international standards.
- The first torsional and lateral modes exhibited high frequencies.
- Resonance phenomena with frequencies of a human-induced load are not expected, since the natural frequencies of the first vertical, lateral, and torsional modes are not close to the typical values of the first and second harmonics of a walking person.
- The high natural frequencies, in spite of the high deformability of the FRP material, are probably due to the type of structure realized, i.e., a spatial truss type that optimizes the use of a composite material excluding the out-of-plane deformation of the structure and preventing the rise of high bending moments.
- A reasonable agreement was obtained between the experimental modal parameters and those extracted from the FE model, which confirmed the results of the experimental modal analysis.
- A comparison with the modal parameters of other footbridges realized with a traditional material or FRP evidenced significantly higher values of frequencies and damping of the bridge considered.
- From results of the dynamic characterization, it can be concluded that, in relation to its dynamic behavior, the analyzed

FRP footbridge performed well. However, an analysis of the dynamic response of the bridge in terms of maximum accelerations under service conditions would also be necessary in order to check the observance of the comfort criteria defined in international standards. In fact, the low mass of the FRP structure could result in a much livelier response in comparison with that of footbridges realized with traditional materials.

REFERENCES

1. J. T. Mottram, "Does performance-based design with FRP components and structures provide any new benefits and challenges?," Structural Engineer, **89**, 23-7 (2011).
2. L. C. Bank, Composites for Construction, Structural Design with FRP Materials, John Wiley and Sons, Inc. (2006).
3. S. Živanović, A. Pavic and P. Reynolds, "Vibration serviceability of footbridges under human-induced excitation: a literature review," J. of Sound and Vibration, **279**, 1-74 (2005).
4. EN 1990, "Eurocode 0 – Basis of structural design", European Committee for Standardization (2002).
5. L. Holloway, Polymer Composites for Civil and Structural Engineering, Chapman & Hall (1993).
6. "Structural plastics design manual," Am. Soc. Civil Engineering Manuals and Reports on Engineering Practice, No. 63. ASCE, NY (1984).
7. A. Di Tommaso and S. Russo, "Shape influence in buckling of GFRP pultruded columns," Mech. Compos. Mater., **39**, No.4, 329-340 (2003).
8. G. Boscato, C. Casalegno, J. T. Mottram, and S. Russo, "Buckling of built-up columns of pultruded fiber-reinforced polymer C-sections," J.of Compos. for Construction, **18** (2014).
9. S. Russo, G. Boscato, and C. Casalegno, "Performance of built-up columns made of a pultruded FRP material," Composite Structures, **121**, 46-63 (2015).
10. S. Russo, "Experimental and finite element analysis of a very large pultruded FRP structure subjected to free vibration," Composites Structures, **94**, 1097-1105 (2012).
11. G. Boscato and S. Russo, "Dissipative capacity of a FRP spatial pultruded structure," Composite Structures, **113**, 339-353 (2014).
12. G. Boscato and S. Russo, "Free vibrations of pultruded FRP elements: Mechanical characterization, analysis, and applications," J. of Compos. for Construction, **13**, 565-574 (2009).
13. G. Boscato, J. T. Mottram, and S. Russo, "Dynamic response of a sheet pile of fiber-reinforced polymer for waterfront barriers," J. of Compos. for Construction, **15**, 974-984 (2011).
14. G. Boscato and S. Russo, "Free vibrations of a pultruded GFRP frame with different rotational stiffnesses of bolted joints," Mech. Compos. Mater., **48**, No. 6, 655-668 (2013).
15. G. Boscato, A. Dal Cin, and S. Russo, "Dynamic identification of All-FRP pultruded structures," Int. J. of Engineering and Technol., **7**, 81-85 (2015).
16. S. Živanović, G. Feltrin, J. T. Mottram, and J. M. W. Brownjohn, "Vibration performance of bridges made of fibre-reinforced polymer," Dynamics of Civil Structures, **4**, 155-162 (2014).
17. Y. Bai and T. Keller, "Modal parameter identification for a GFRP pedestrian bridge," Composite Structures, **82**, 90-100 (2008).
18. A. J. Aref and S. Alampalli, "Vibration characteristics of a fiber-reinforced polymer bridge superstructure," Composite Structures, **52**, 467-474 (2011).
19. R. Burgueño, V. M. Karbhari, F. Seible, and R. T. Kolozs, "Experimental dynamic characterization of an FRP composite bridge superstructure assembly," Compos. Struct., **54**, 427-444 (2001).
20. J. N. Juang and R. S. Pappa, "An eigensystem realization algorithm for modal parameter identification and model reduction," J. of Guidance, Control and Dynamics, **8**, 620-627 (1977).